Periodic trends in the structural, electronic and transport properties of electrenes

Mohammad Rafiee Diznab,[†] Erin R. Johnson,[*,†,‡] and Jesse Maassen[*,†]

[†]*Department of Physics and Atmospheric Science, Dalhousie University, Halifax, Nova Scotia B3H 4R2, Canada*

[‡]*Department of Chemistry, Dalhousie University, Halifax, Nova Scotia B3H 4R2, Canada*

E-mail: erin.johnson@dal.ca; jmaassen@dal.ca

1 Landauer transport formalism

1.1 Mathematical expressions

The electrical conductivity within a Landauer transport framework[1] can be defined as

$$\sigma = \left(\frac{2q^2}{h}\right) I_0 \,, \tag{1}$$

where σ is the electrical conductivity, q is carrier charge, h is Planck's constant and the quantity I_0 is written as

$$I_0 = \frac{h}{2} \int_{-\infty}^{+\infty} \Sigma(E) \left(-\frac{\partial f_0}{\partial E}\right) dE, \tag{2}$$

where $\Sigma(E)$ is the transport distribution as a function of energy, E, μ is the Fermi level, k_B is Boltzmann's constant, T is temperature, and f_0 is the Fermi-Dirac distribution. The

transport distribution function can be expressed as

$$\Sigma(E) = \frac{1}{\Omega} \sum_{k,s,n} \nu_x^2(k)\, \tau(k)\, \delta[E - \epsilon(k)],^{1} \tag{3}$$

where the sum runs over all k points in the Brillouin zone, spin states s, and band index n. Here, Ω is the sample volume, $\epsilon(k)$ is the electronic dispersion (i.e. band structure), $\tau(k)$ is the scattering time and $\nu_x = 1\hbar\,(\partial\epsilon\partial k_x)$ is the group velocity along the direction of transport (here assumed to be the $\hat{x}$ direction). Since $\Sigma(E)$ contains all material properties, it is considered the central quantity in these calculations.

Next, we re-arrange $\Sigma(E)$ to express it as the product of two physically-intuitive quantities, the distribution-of-modes ($M(E)$) and mean-free-path for backscattering ($\lambda(E)$). The resulting $\Sigma(E)$ is

$$\Sigma(E) = \frac{2}{h}\, M(E)\, \lambda(E). \tag{4}$$

From a physical perspective, the distribution-of-modes (or DOM) represents the number of conducting channels available for transport, and is defined as

$$M(E) = \frac{h}{4\Omega} \sum_{k,s,n} |\nu_x(k)|\, \delta[E - \epsilon(k)]. \tag{5}$$

The other physically descriptive quantity is the mean-free-path for backscattering. $\lambda(E)$, which quantifies the average distance along the transport direction before the ν_x component of electrons changes sign due to scattering, and is defined as

$$\lambda(E) = 2\, \frac{\sum_{k,s,n} \nu_x^2(k)\, \tau(k)\, \delta[E - \epsilon(k)]}{\sum_{k,s,n} |\nu_x(k)|\, \delta[E - \epsilon(k)]}. \tag{6}$$

Since the relaxation time is assumed to be a function of energy in this work, we can write

[1] Note that the explicit s and n dependence of the quantities in Eq. (3) is omitted for clarity.

the $\lambda(E)$ as a product of the average velocity of carriers, V_λ, and the relaxation time, $\tau(E)$:

$$\lambda(E) \;=\; V_\lambda(E)\,\tau(E), \tag{7}$$

where V_λ is defined as

$$V_\lambda(E) = 2\,\frac{\sum_{k,s,n}\nu_x^2(k)\,\delta[E-\epsilon(k)]}{\sum_{k,s,n}|\nu_x(k)|\,\delta[E-\epsilon(k)]}. \tag{8}$$

In this case, the transport distribution takes on the following form

$$\Sigma(E) = \frac{2}{h}M(E)\,V_\lambda(E)\,\tau(E). \tag{9}$$

The scattering rates is assumed to be proportional to the DOS, such that $\tau(E) = k_0/\,D(E)$, so the transport distribution can be expressed as

$$\Sigma_{DOS}(E) = \frac{2}{h}M(E)\,V_\lambda(E)\,\frac{k_0}{D(E)}\,, \tag{10}$$

where k_0 is an adjustable parameter.

1.2 Density of states, average velocity, and distribution of modes

The calculated electronic density of states, $D(E)$, averaged carrier velocities, $\langle \nu_x^+ \rangle$, and distribution of modes, $M(E)$, for all monolayer and bilayer electrenes can be found in Fig. S1-S4. The plotted average velocity is defined as

$$\langle \nu_x^+ \rangle = \frac{\sum_{k,s,n} |\nu_x(k)| \, \delta[E - \epsilon(k)]}{\sum_{k,s,n} \delta[E - \epsilon(k)]}. \tag{11}$$

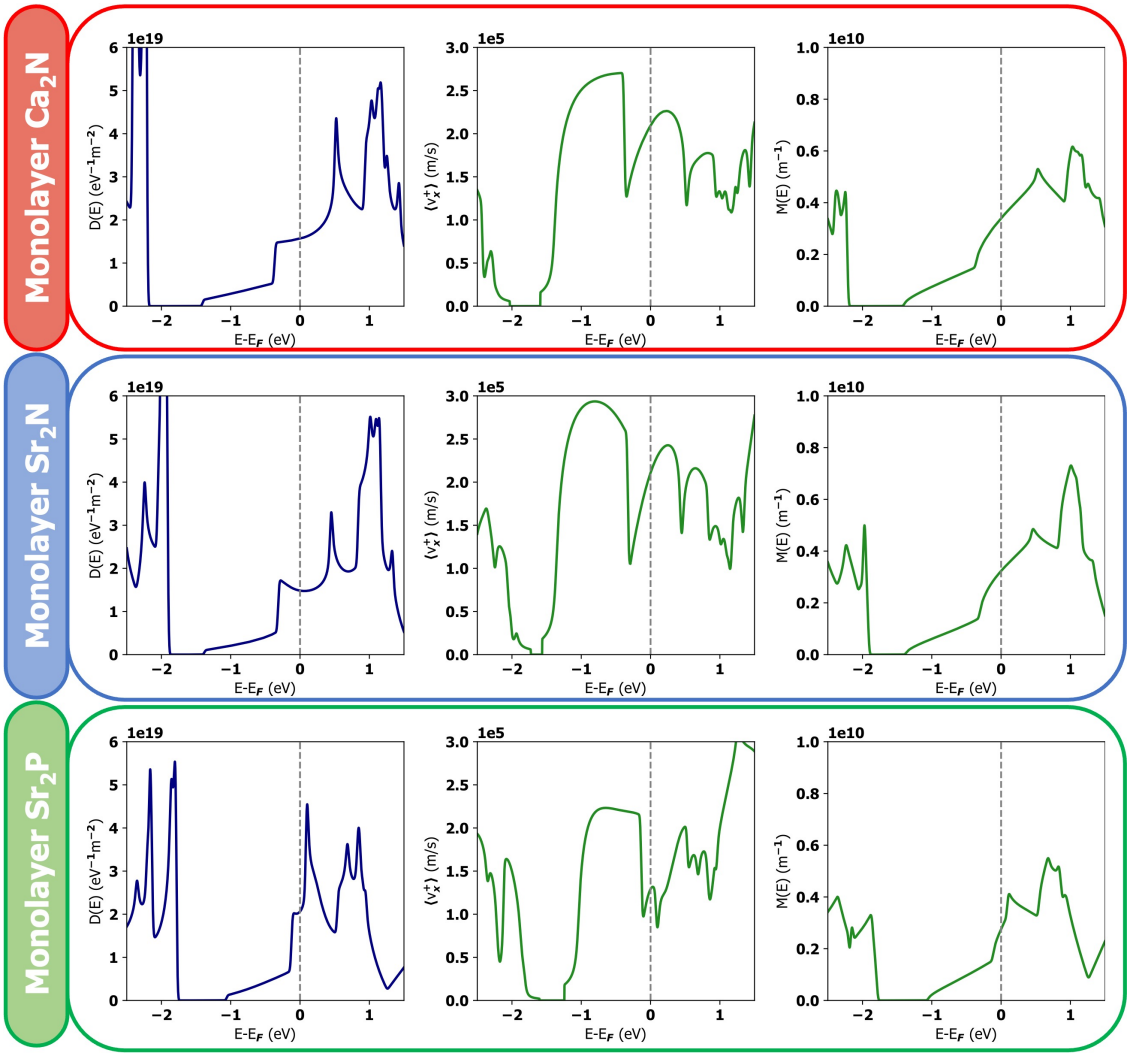

Fig. S 1: Calculated DOS (left), averaged velocity (center), and DOM (right) for monolayer Ca_2N, Sr_2N and Sr_2P.

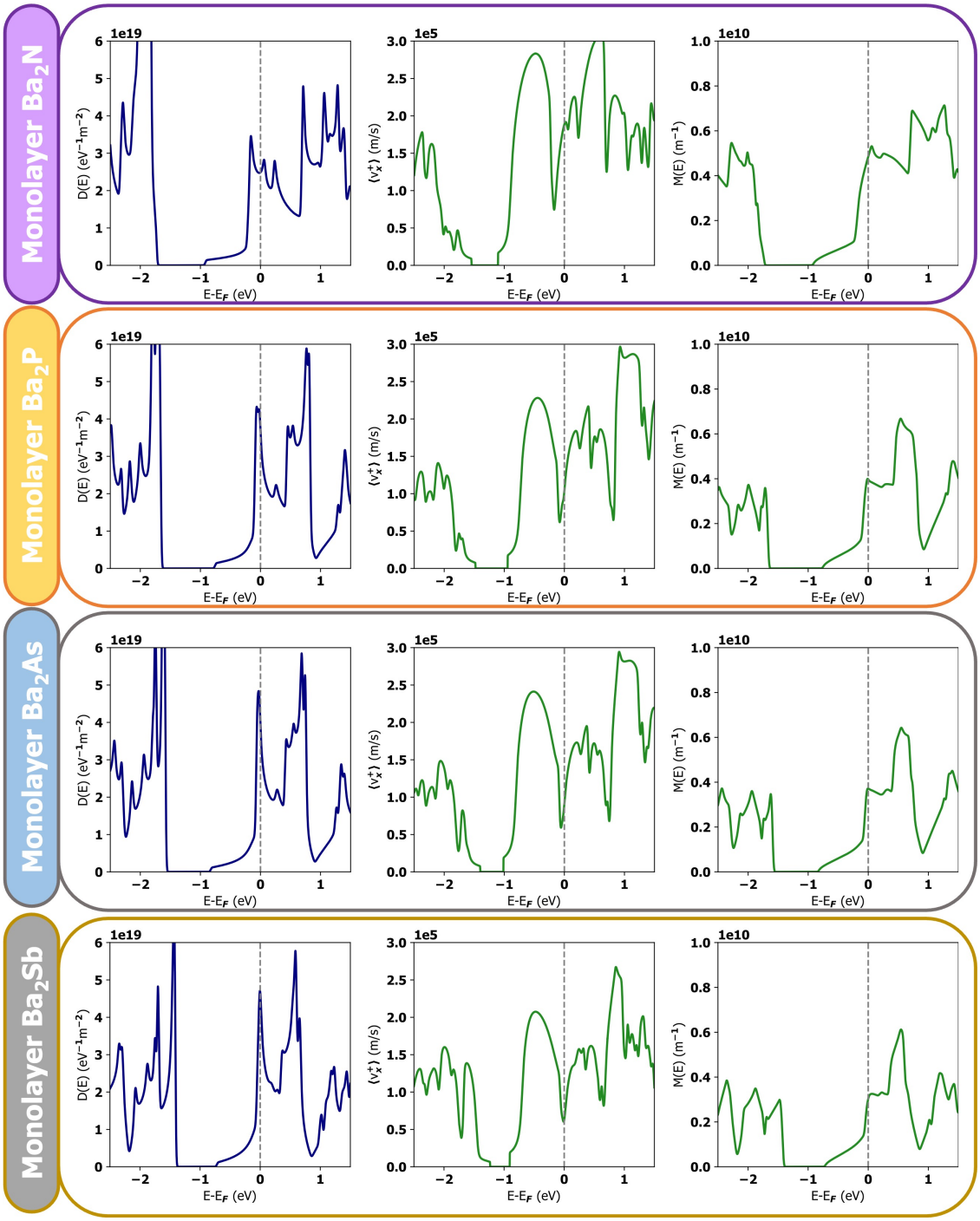

Fig. S 2: Calculated DOS (left), averaged velocity (center), and DOM (right) for monolayer Ba_2N, Ba_2P, Ba_2As and Ba_2Sb.

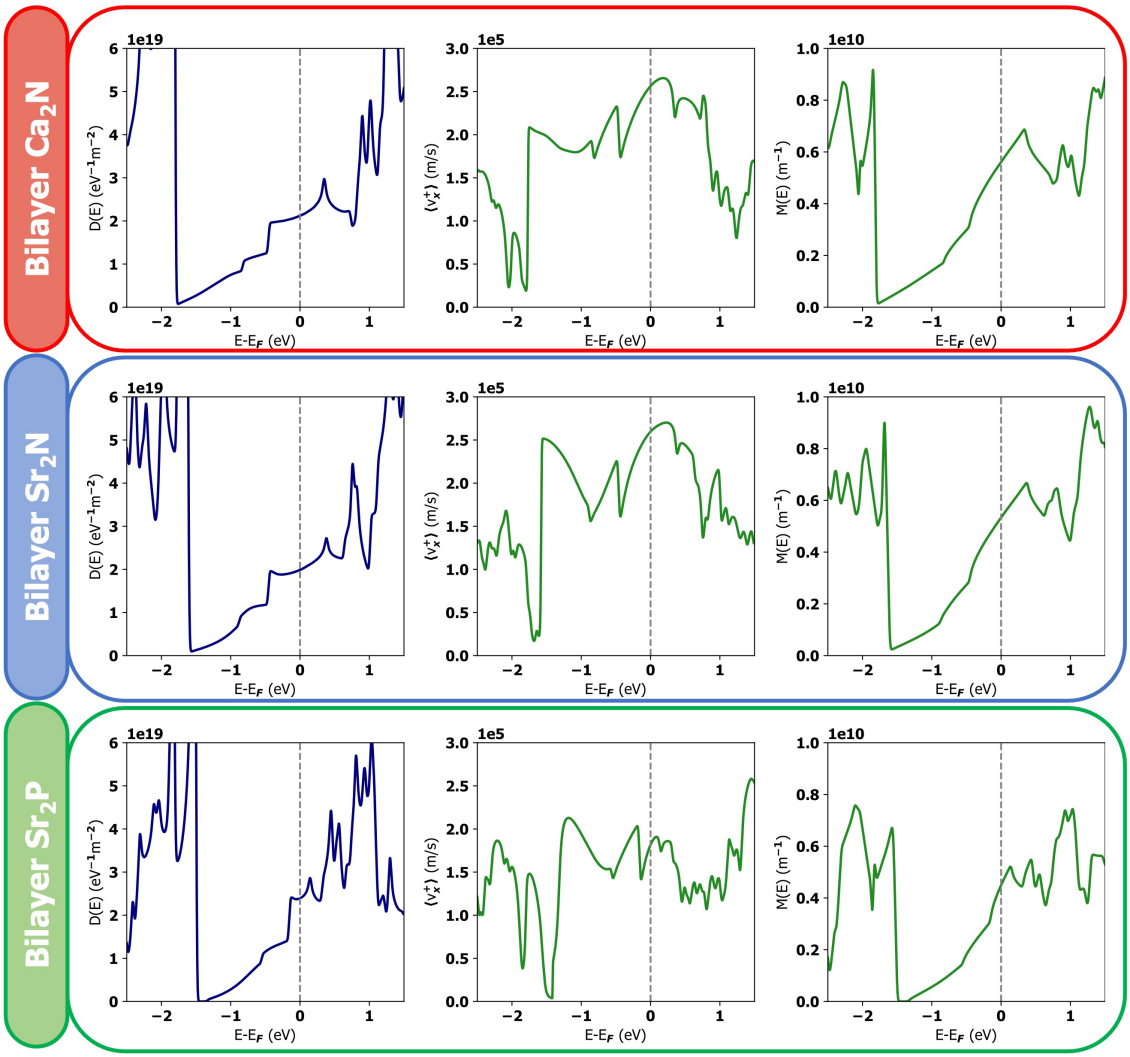

Fig. S 3: Calculated DOS (left), averaged velocity (center), and DOM (right) for bilayer Ca_2N, Sr_2N and Sr_2P.

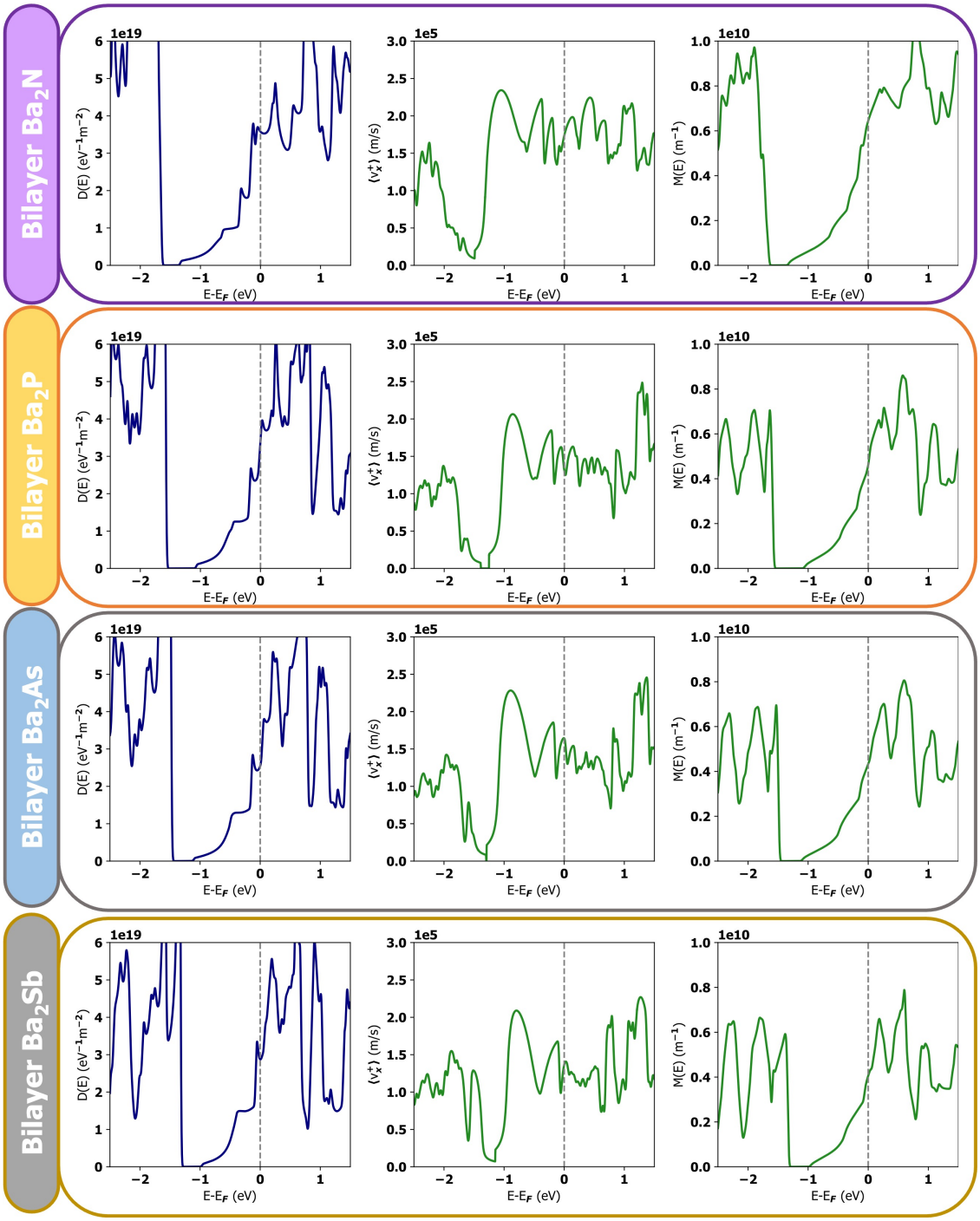

Fig. S 4: Calculated DOS (left), averaged velocity (center), and DOM (right) for bilayer Ba_2N, Ba_2P, Ba_2As and Ba_2Sb.

2 Transport properties

2.1 Rigorous electron-phonon scattering in monolayer Ca_2N

The value of the proportionality constant, k_0, was determined by matching the Landauer conductivity of monolayer Ca_2N to that obtained using `Perturbo`[2] (with **k**- and **q**- grids of 200×200×1), which captures the detailed electron-phonon scattering rates. The fitted value of $k_0 = 9.13\times10^4$ $eV^{-1}\,m^{-2}\,s$ was obtained for monolayer Ca_2N.

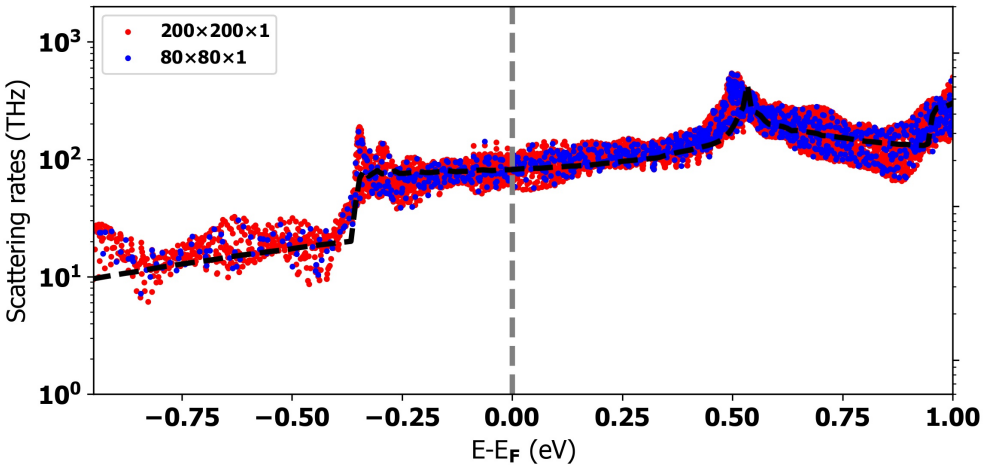

Fig. S 5: Electron-phonon scattering rates of Ca_2N monolayers using fine 200×200×1 and 80×80×1 **k**-point and **q**-point grids. The dashed line shows the energy-dependent DOS scattering rates.

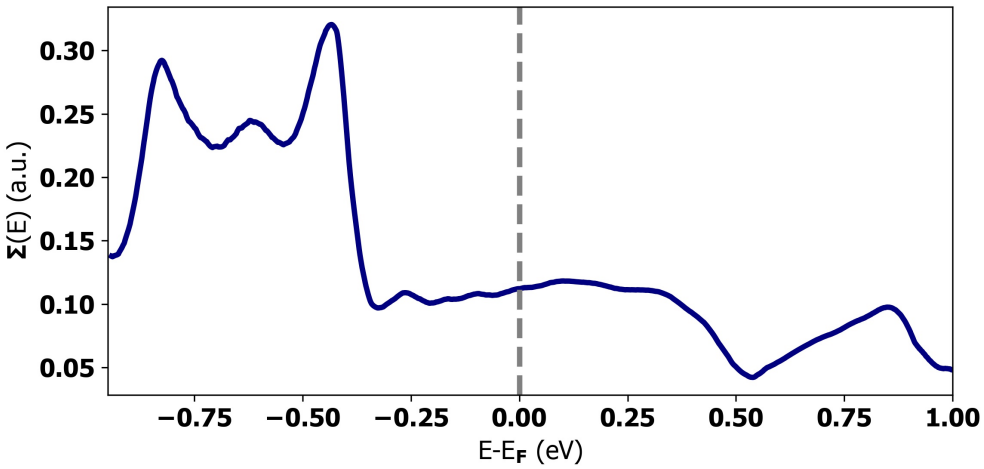

Fig. S6: Computed transport distribution function (TDF) of monolayer Ca_2N obtained from rigorous electron-phonon calculations. An abrupt drop in the TDF is observed near -0.4 eV, which corresponds to an increase in the DOS arising from the band edge of the upper surface band.

3 Lattice parameters, exfoliation energies, and work functions without dispersion correction

Table S 1: Calculated monolayer (a_m) and bilayer (a_b) lattice constants and interlayer distance of bilayer structures (c_b) without the D3(BJ) dispersion correction.

	a_m (Å)				a_b (Å)				c_b (Å)		
	Ca	Sr	Ba		Ca	Sr	Ba		Ca	Sr	Ba
N	3.61	3.86	4.01	N	3.61	3.86	4.03	N	3.73	4.08	4.83
P	-	4.45	4.66	P	-	4.69	4.65	P	-	3.99	4.45
As	-	-	4.76	As	-	-	4.77	As	-	-	4.40
Sb	-	-	5.02	Sb	-	-	5.03	Sb	-	-	4.25

Table S 2: Exfoliation energies of electrenes without the D3(BJ) dispersion correction.

	E_{exfo} (meV/Å^2)		
	Ca	Sr	Ba
N	70	54	38
P	-	42	31
As	-	-	30
Sb	-	-	27

Table S 3: Monolayer and bilayer work functions ($\Phi_m^{monolayer}$ and $\Phi_m^{bilayer}$) without the D3(BJ) dispersion correction.

	$\Phi_m^{monolayer}$ (eV)				$\Phi_m^{bilayer}$ (eV)		
	Ca	Sr	Ba		Ca	Sr	Ba
N	3.58	3.35	3.01	N	3.40	3.15	3.00
P	-	2.98	2.68	P	-	2.78	2.66
As	-	-	2.62	As	-	-	2.59
Sb	-	-	2.48	Sb	-	-	2.40

4 Electron localization function (ELF)

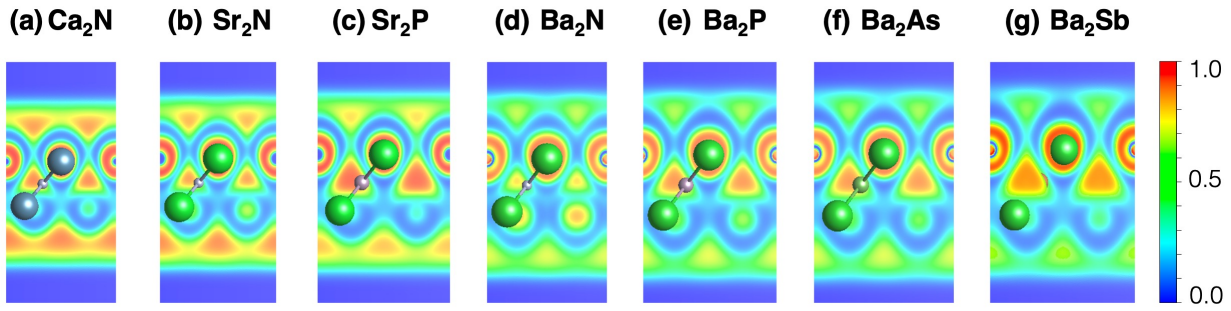

Fig. S 7: Electron localization function (ELF) of monolayer electrenes. The ELF values are mapped onto a range between 0 and 1, where 1 corresponds to perfect localization and 0.5 is comparable to a uniform electron gas. The extent of electron localization at the surfaces is increased, compared to the central region of the atomic layer, for lighter elements.

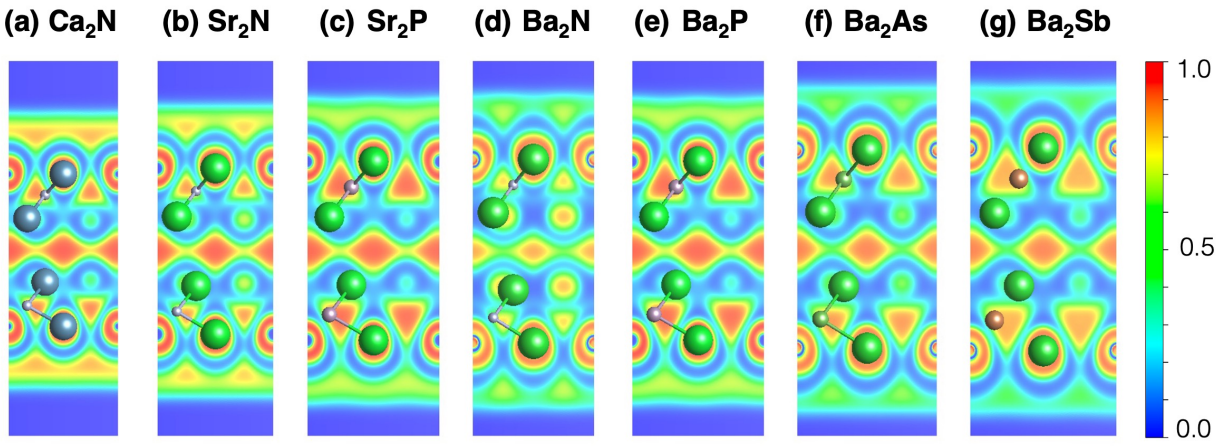

Fig. S 8: Electron localization function (ELF) of bilayer electrenes. The colour bar indicates the range of values between 0 and 1. Similar to the monolayers, the surface states are more localized for lighter elements.

5 Crystal orbital Hamilton population (COHP)

Table S 4: Integrated crystal orbital Hamilton population (IpCOHP) for monolayer electrenes.

	-IpCOHP$^{\text{Total}}$ ($\times 10^{-1}$)				-IpCOHP^{s-s} ($\times 10^{-1}$)				-IpCOHP$^{s-p_z}$ ($\times 10^{-1}$)		
	Ca	Sr	Ba		Ca	Sr	Ba		Ca	Sr	Ba
N	3.75	3.32	2.56	N	1.09	0.94	0.95	N	0.64	0.43	0.14
P	-	3.50	2.95	P	-	0.82	0.91	P	-	0.66	0.33
As	-	-	3.02	As	-	-	0.84	As	-	-	0.37
Sb	-	-	3.10	Sb	-	-	0.80	Sb	-	-	0.42

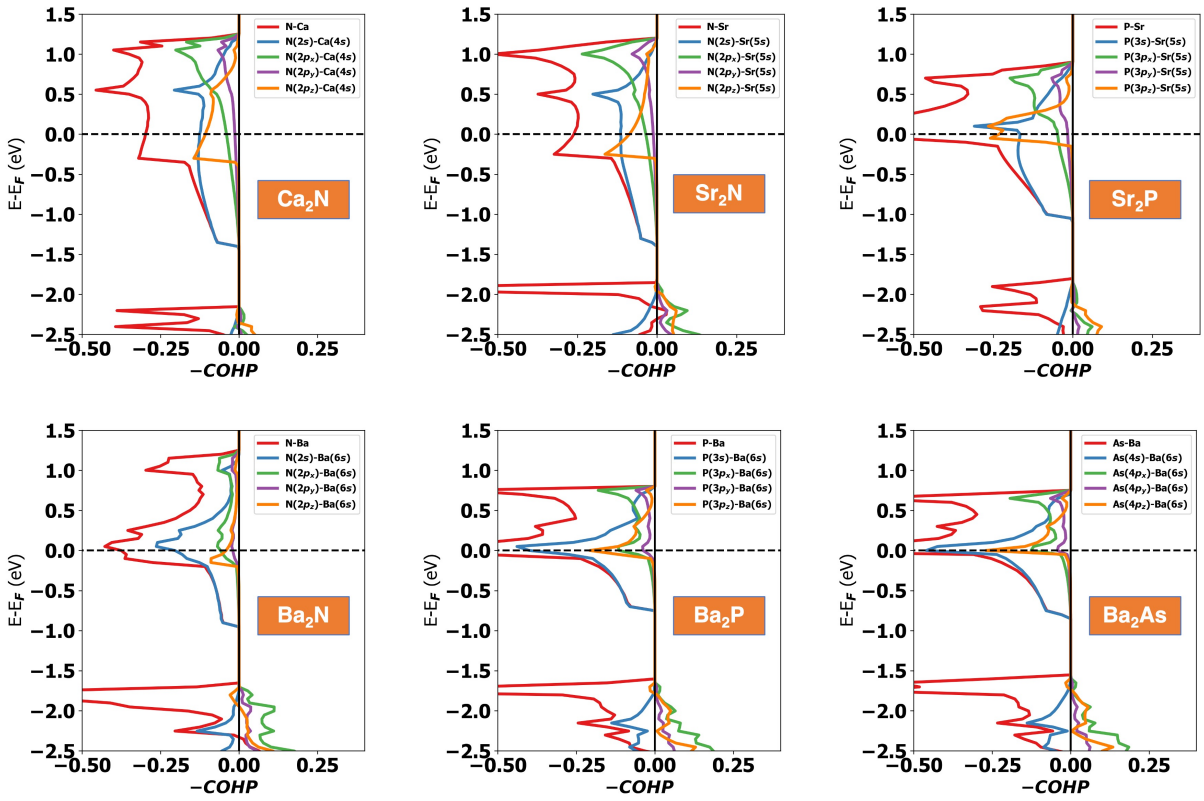

Fig. S 9: Orbital-wise COHP plots for the monolayer electrenes.

6 Bader charges

Table S 5: Calculated Bader charges of monolayer electrides. The left and right panels show the charges for the alkaline earth metals and the pnictogens, respectively.

	$Q^{\text{Metal}}_{\text{Bader}}$ (e)				$Q^{\text{Pnictogen}}_{\text{Bader}}$ (e)		
	Ca	Sr	Ba		Ca	Sr	Ba
N	1.07	1.00	0.87	N	2.14	2.00	1.75
P	-	1.10	0.94	P	-	2.21	1.89
As	-	-	0.94	As	-	-	1.88
Sb	-	-	0.96	Sb	-	-	1.93

7 Convergence tests

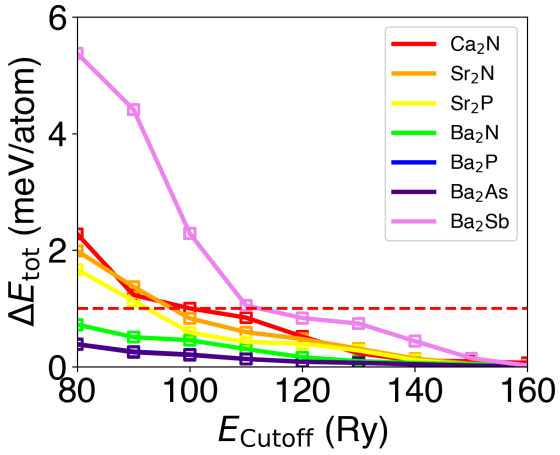

Fig. S 10: Change in the total energy with respect to increasing cutoff energy for all studied monolayers.

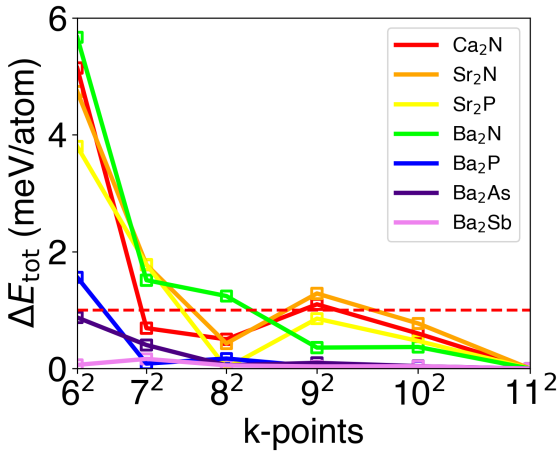

Fig. S 11: Change in the total energy with respect to increasing **k**-point density for all studied monolayers.

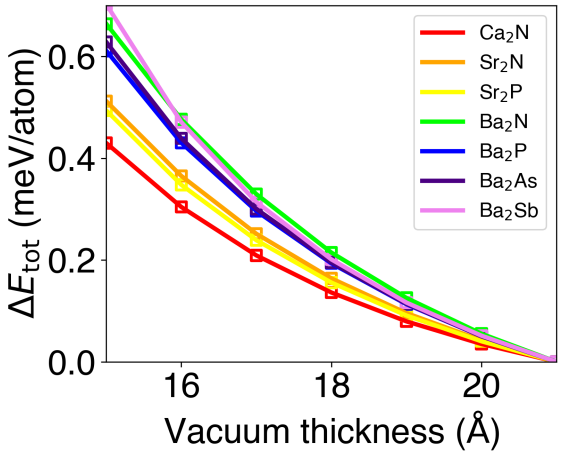

Fig. S 12: Change in the total energy with respect to increasing vacuum thickness for all studied monolayers.

8 Band structure of Ca_2N with experimental lattice constant

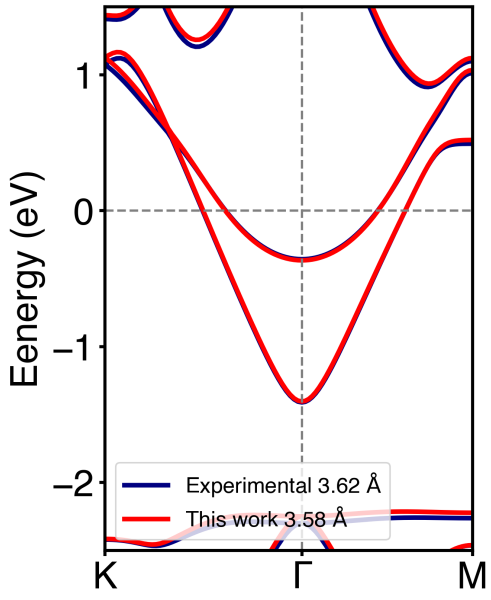

Fig. S 13: Electronic structure of monolayer Ca_2N with the experimental lattice constant[3] of 3.62 Å and the DFT-calculated lattice constant of 3.58 Å.

9 Phonon dispersion of electrenes

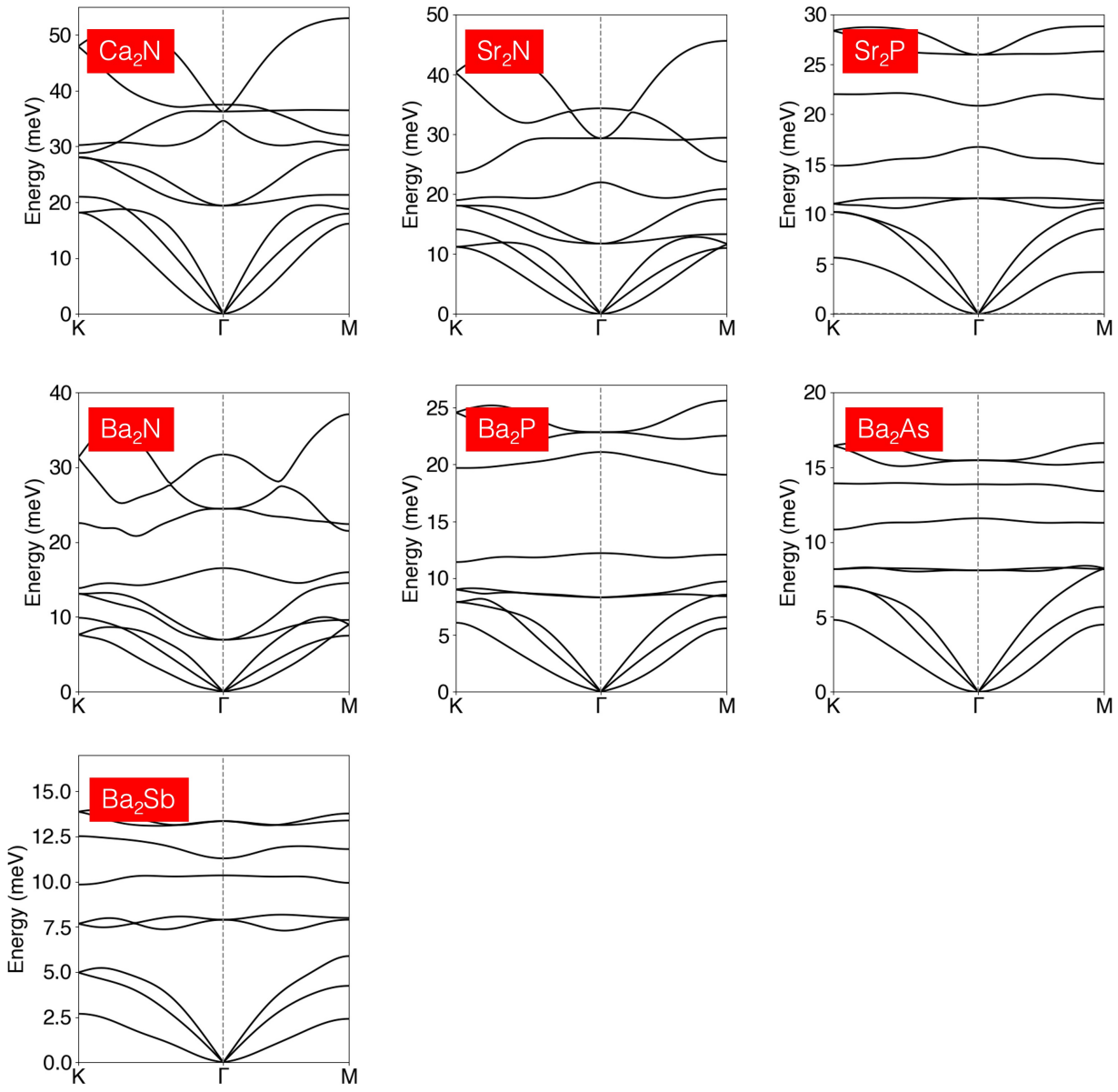

Fig. S 14: Phonon dispersion of monolayer electrenes. No negative phonon energies are observed, indicating the dynamical stability of these materials. Calculations were performed using DFPT, a q-grid of 8×8×1 for Ca_2N and Sr_2N, 10×10×1 for Ba_2N and 5×5×1 for the rest of the materials. In all cases, a convergence threshold of 10^{-20} was used for self-consistency calculations.

10 References

(1) Rudderham, C.; Maassen, J. Ab initio thermoelectric calculations of ring-shaped bands in two-dimensional Bi_2Te_3, Bi_2Se_3, and Sb_2Te_3: Comparison of scattering approximations. *Physical Review B* **2021**, *103*, 165406.

(2) Zhou, J.-J.; Park, J.; Lu, I.-T.; Maliyov, I.; Tong, X.; Bernardi, M. Perturbo: A software package for ab initio electron–phonon interactions, charge transport and ultrafast dynamics. *Computer Physics Communications* **2021**, *264*, 107970.

(3) Druffel, D. L.; Kuntz, K. L.; Woomer, A. H.; Alcorn, F. M.; Hu, J.; Donley, C. L.; Warren, S. C. Experimental Demonstration of an Electride as a 2D Material. *Journal of the American Chemical Society* **2016**, *138*, 16089–16094.